Numerical Simulation of Flying Phenomena of the Running Tape on Rotating Drum

Oakkey Min* and Haesung Kwon**

(Received May 10, 1993)

This paper analyzes the running mechanism of flexible and thin tape above rotating protrusion through a numerical simulation. The scope of analysis is confined to the phenomena of elastohydrodynamic lubrication between the rotating drum with a protrusion and the running tape. This model is based on the modified Reynolds equation and the equation of plate considering the effect of geometric nonlinearity and geometry of protrusion. Finite element method of Bubnov- Galerkin type is adopted as a numerical simulation technique to solve the above two coupled nonlinear equations. In numerical simulation, the influences of tape tension and protrusion velocity are evaluated in simple model. In complex models, the reciprocal action of two protrusions is simulated.

Key Words: Elasto-Hydrodynamic Lubrication, Finite Element Method, Modified Reynolds Equation

1. Introduction

In the magnetic-recording device, the hydrodynamic pressure is produced by relative velocity between protrusion and running tape. The flying characteristics of tape make infinitesimal spacing between magnetic tape and rotating protrusion and prevent wear, but produce spacing loss between protrusion and tape and decrease the output of recording or reproduction signal. It is essential to maintain the proper spacing between rotating protrusion and tape which is running with uniform relative velocty above the infinitesimally protruded magnetic protrusion on circumferential plane of drum rotating with high speed. The contact of rotating part of drum and tape is undesirable of reliability and durability of system, and produces the variation of the output signal from the protrusion and yields bad effects on the quality of reproduced signal. Therefore, there is a need to elucidate the flying characteristic of tape over the drum.

The studies on flying characteristics of thin foil were carried out in the computer magnetic disk device and magnetic tape device by the simple theoretical model(Giro et al., 1969) and the finite difference method(Langlois, 1975). The Fourier series and nonuniform finite difference scheme were used to solve tape displacement and pressure distribution, respectively(Wolf et al., 1983). The finite element scheme, which was applied to 8mm camcorder running system, was introduced showing overall flying characteristics of tape over drum with point protrusion(Yoneda et al., 1988). The mutual interference between heads and tapes in VCR's is performed when plural heads are adjacent positions using finite difference method (Sakai et al., 1990). The orthotropic material property was considered in the linear elasticity equation of tape(Kotera et al., 1991). The correction factor was adopted to describe the tape stiffness pertinently using finite difference method(Min et al., 1991). In order to depict the stiffness of tape accurately, the governing equation of tape model was chosen for a finite-width thin plate considering geometrical nonlinearity. And the numerical study was performed accord-

* Department of Mechanical Design and Production Engineering, Yonsei University, Seoul, Korea
** Deparatment of Mechanical Engineering, Graduate School, Yonsei University, Seoul, Korea

ing to system parameter-relative veloctiy (Kim et al., 1992).

In this paper, the procedure of numerical analysis is formulated by using finite element scheme for the plate equation and the modified Reynolds equation. Tape tension and relative velocity between flying tape and rotating protrusion are considered as the principal parameters of simulations. To understand the behavior of tape more closely, a numerical analysis is carried out over the finite region of tape around the protrusion.

2. Elastohydrodynamic Lubrication Mechanism

The elastohydrodynamic lubrication mechanism caused by the relative high speed between the running tape and protrusion on rotating drum is formulated. In case of the tape running over rotating drum, displacement of tape is determined mainly by the geometrical shape of protrusion, tape tension and relative velocity. In elastohydrodynamic mechanism, the displacement of tape and the pressure of air gap are coupled with flying height between tape and drum running with relative velocity.

2.1 Elasticity equation

The differential equations about the displacements U,V and W of tape are based on the nonlinear elastic plate theory considering large displacement in middle plane of tape. The assumptions are as follows,

① Tension variation by viscous friction of lubricants is neglected.

② The inertia term is neglected.

③ In-plane stress in the tape, i.e., geometric nonlinearity is described to the second term.

④ The damping term of thin foil is not included.

⑤ Friction force by contact is neglected.

and the governing relations are given by Eqs. (1), (2) and (3) as

$$g_u \equiv \frac{\partial \sigma_x}{\partial x} + \frac{\partial \sigma_{xy}}{\partial y} = 0 \tag{1}$$

$$g_v \equiv \frac{\partial \sigma_{xy}}{\partial x} + \frac{\partial \sigma_y}{\partial y} = 0 \tag{2}$$

$$g_w \equiv D_1\left(\frac{\partial^4 W}{\partial x^4} + \frac{\partial^4 W}{\partial y^4} + 2\frac{\partial^4 W}{\partial x^2 \partial y^2}\right) - \left(\sigma_x \frac{\partial^2 W}{\partial x^2} + \sigma_y \frac{\partial^2 W}{\partial y^2} + 2\sigma_{xy}\frac{\partial^2 W}{\partial x \partial y}\right) - (P_a - p(x, y)) = 0 \tag{3}$$

$$\begin{pmatrix} \sigma_x \\ \sigma_y \\ \sigma_{xy} \end{pmatrix} = D_2 \begin{bmatrix} 1 & \nu & 0 \\ \nu & 1 & 0 \\ 0 & 0 & (1-\nu)/2 \end{bmatrix} \begin{pmatrix} \varepsilon_x \\ \varepsilon_y \\ \varepsilon_{xy} \end{pmatrix} \tag{4}$$

$$\begin{pmatrix} \varepsilon_x \\ \varepsilon_y \\ \varepsilon_{xy} \end{pmatrix} = \begin{bmatrix} U,_x + (1/2)(W,_x)^2 \\ V,_y + (1/2)(W,_y)^2 \\ U,_y + V,_x + (W,_x)(W,_y) \end{bmatrix} \tag{5}$$

$$D_1 = \frac{Et^3}{12(1-\nu^2)},\quad D_2 = \frac{Et}{(1-\nu^2)}$$

where W is the out-of-plane(z) displacement of tape, U and V are displacements in longitudinal(x) and transverse(y) directions respectively. The absolute pressure and the ambient pressure are denoted by p and P_a. Young's modulus E and Poisson's ratio ν are defined isotropically. Equations (4) and (5) give the relation of in-plane stress components σ_x, σ_y and σ_{xy} of the tape to the displacements considering isotropic geometrical nonlinearity.

2.2 Modified Reynolds equation

Lubrication of the spacing and pressure distribution is based on the assumptions as follows,

① The lubrication spacing and pressure distribution are in steady-state.

② Lubricants is laminar.

③ Inertia effect of lubricants is neglected.

④ Temperature variation of lubricants is neglected and viscosity of fluid is uniform and regular.

⑤ Spacing is normal to the direction of the middle plane of tape.

The modified Reynolds equation derived from Navier-Stokes equation and continuity as

$$g_p \equiv \mathrm{div}(h^3 p\ \mathrm{grad}\ p) + 6\lambda_a p_a (h^2 \mathrm{grad}\ p) - 6\mu_a \mathrm{div}(\mathrm{phv}) = 0 \tag{6}$$

Here, v is the relative velocity between tape and protrusion, λ_a is mean free path of air molecule in standard temperature and pressure, μ_a is coefficient of viscosity, and h is spacing. As the spacing between protrusion and tape of magnetic recording device would be sub-micron magnitude, modified Reynolds equation is used.

2.3 Compatibility equation

The quantity of flying height, resulted in the spacing effect of thin tape produced by the air

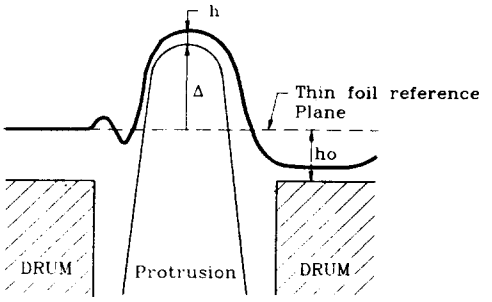

Fig. 1 Typical relation between tape, drum and protrusion

lubrication, is determined by the displacement of tape and the shape of protrusion and drum as,

$$h=h_0+W-\Delta \tag{7}$$

where the vertical displacement W of elasticity equation and the spacing h of lubrication equation are related to geometrical shape of protrusion Δ and initial spacing h_0 between tape, drum and protrusion is shown in Fig. 1.

2.4 Boundary conditions

The boundary conditions applied to the lubrication equation and the elasticity equations are written as

$$m_u\equiv\sigma_x n_x+\sigma_{xy}n_y-F_x=0 \quad \text{on } S_u \tag{8}$$

$$m_v\equiv\sigma_{xy}n_x+\sigma_y n_y-F_y=0 \quad \text{on } S_v \tag{9}$$

$$\begin{aligned} m_1\equiv&\frac{\partial}{\partial S}\Big[(\frac{\partial^2 W}{\partial x^2}+\nu\frac{\partial^2 W}{\partial y^2})n_x n_y\\ &-(1-\nu)\frac{\partial^2 W}{\partial x\partial y}(n_x^2-n_y^2)\\ &-(\frac{\partial^2 W}{\partial y^2}+\nu\frac{\partial^2 W}{\partial x^2})n_x n_y\Big]\\ &-\frac{\partial}{\partial x}(\frac{\partial^2 W}{\partial x^2}+\frac{\partial^4 W}{\partial y^4})n_x\\ &-\frac{\partial}{\partial y}(\frac{\partial^2 W}{\partial y^2}+\frac{\partial^2 W}{\partial x^2})n_y=0 \quad \text{on } S_1 \end{aligned} \tag{10}$$

$$\begin{aligned} m_2\equiv&\Big[(\frac{\partial^2 W}{\partial x^2}+\nu\frac{\partial^2 W}{\partial y^2})n_x^2\\ &+2(1-\nu)\frac{\partial^2 W}{\partial x\partial y}n_x n_y\\ &+(\frac{\partial^2 W}{\partial y^2}+\nu\frac{\partial^2 W}{\partial x^2})n_y^2\Big]=0 \quad \text{on } S_2 \end{aligned} \tag{11}$$

$$\begin{aligned} m_3\equiv&(\sigma_x\frac{\partial W}{\partial x}+\sigma_{xy}\frac{\partial W}{\partial y})n_x\\ &+(\sigma_y\frac{\partial W}{\partial y}+\sigma_{xy}\frac{\partial W}{\partial x})n_y=0 \quad \text{on } S_3 \end{aligned} \tag{12}$$

$$m_4\equiv W-W_0=0 \quad \text{on } S_W \tag{13}$$

$$\begin{aligned} m_{p1}\equiv&[(h^3 p+6\lambda_a p_a h^2)\cdot\text{grad } p\\ &-6\mu_a(ph\cdot V)]\cdot n=0 \quad \text{on } S_{p1} \end{aligned} \tag{14}$$

$$m_{p2}\equiv p-p_a=0 \quad \text{on } S_{pa} \tag{15}$$

where m_u is the load boundary condition(B.C.) at the edge of tape in tape-length direction(Su), m_v is the load B.C. at the edge of tape in tape-width direction(Sv), m_1 is the shear force B.C. caused by the moment acting along the boundary of tape(S_1), m_2 is the moment B.C. acting along the boundary of tape(S_2), m_3 is the inplane force B.C. acting along boundary of tape(S_4), m_4 is displacement B.C. at the end of tape(S_4), m_{p1} is fluid quantity B.C. of the air lubrication layer at the edge of tape(S_{p1}) and m_{p2} is the pressure B.C. of the air lubrication layer at the edge of tape(S_{p2}).

2.5 Application of finite element method

In numerical analysis, displacements U, V, W and pressure p in a triangular element are approximated as

$$U(x,y)\cong\hat{U}(x,y)=\sum_{m=1}^{3}N_m^u(x,y)u_m \tag{16}$$

$$V(x,y)\cong\hat{V}(x,y)=\sum_{m=1}^{3}N_m^v(x,y)v_m \tag{17}$$

$$W(x,y)\cong\hat{W}(x,y)=\sum_{m=1}^{3}N_m^w(x,y)w_m \tag{18}$$

$$p(x,y)\cong\hat{p}(x,y)=\sum_{m=1}^{3}N_m^p(x,y)p_m \tag{19}$$

where N_m^u and N_m^v are the inplane displacement shape function, N_m^w is the vertical displacement shape function and N_m^p is the pressure shape function. u_m, v_m, w_m and p_m are the vectors defined on the nodal point m.

2.6 Solution schemes of nonlinear equations

Applying the weighted residual method of Bubnov-Galerkin type to governing equations(g_u, g_v, g_w, g_p) and the boundary conditions(m_u, m_v, m_1, m_2, m_3, m_4, m_{p1}, m_{p2}), Eqs. (20)~(23) are then given by

$$G_u\equiv\int_R g_u N^u dR+\int_{s\,u} m_u N^u dS \tag{20}$$

$$G_v\equiv\int_R g_v N^v dR+\int_{s\,v} m_v N^v dS \tag{21}$$

$$\begin{aligned} G_w\equiv&\int_R g_w N^w dR+\int_{s\,1} m_1 N^w dS\\ &+\int_{s\,2} m_2 N^w dS+\int_{s\,3} m_3 N^w dS\\ &+\int_{s\,4} m_4 N^w dS \end{aligned} \tag{22}$$

$$G_p \equiv \int_R g_p N^p dR + \int_{sp1} m_{p1} N^p dS + \int_{sp2} m_{p2} N^p dS \quad (23)$$

where R is the region except the boundary and N_u, N_v, N_w and N_p are the weighting function defined in the region R and on the boundary S. The global systems, G_u, G_v, G_w and G_p are composed of the set of simultaneous nonlinear equations. Hence, the Newton-Raphson method, nonlinear solution scheme, is adopted. The tangent stiffness matrix $[\partial G/\partial Q]$ and the residuals $\{G\}$ are constituted as Eq. (24) by linearizing global system equations.

$$\left[\frac{\partial G}{\partial Q}\right]^n \{\Delta Q\}^n = \{-G\}^n$$
$$\{Q\}^{n+1} = \{Q\}^n + R_f \{\Delta Q\}^n$$
$$\{Q\} = \{u_i,\ v_i,\ w_i,\ \theta_{xi},\ \theta_{yi},\ \theta_{zi},\ p_i\} \quad i = 1, 2, 3$$
$$\left[\frac{\partial G}{\partial Q}\right] = \begin{bmatrix} \frac{\partial G_u}{\partial u_m} & \frac{\partial G_u}{\partial v_m} & \frac{\partial G_u}{\partial w_m} & \frac{\partial G_u}{\partial p_m} \\ \frac{\partial G_v}{\partial u_m} & \frac{\partial G_v}{\partial v_m} & \frac{\partial G_v}{\partial w_m} & \frac{\partial G_v}{\partial p_m} \\ \frac{\partial G_w}{\partial u_m} & \frac{\partial G_w}{\partial v_m} & \frac{\partial G_w}{\partial w_m} & \frac{\partial G_w}{\partial p_m} \\ \frac{\partial G_p}{\partial u_m} & \frac{\partial G_p}{\partial v_m} & \frac{\partial G_p}{\partial w_m} & \frac{\partial G_p}{\partial p_m} \end{bmatrix}$$
$$\{G\}^T = \{G_u\ G_v\ G_w\ G_p\} \quad (24)$$

The superscript n is the iteration step of the calculation, $\{Q\}$ is the nodal displacements and the pressure, $\{Q\}^{n+1}$ is the new value of degree of freedoms for the next solution step. $\{\Delta Q\}$ is the corrections of each degree of freedom calculated at the current iteration step. R_f is the relaxation factor. The convergence indicator, ε is defined in Eq. (25)

$$\varepsilon = \Sigma|\Delta Q_i| / \Sigma|Q_i| \quad (25)$$

where summations are performed over the total d.o.f. of the model. In this paper, considering calculation time, the solution is decided to be converged when ε is below $10^{-3} \sim 10^{-4}$ depending on the model.

3. Results and Discussion

Two numerical models are selected. One is the simple model with one protrusion and coarse element topology, and the other is the complex model with two protrusions and dense element topology. In the simple model, the effects of two major parameters in tape running system(tape tension and relative velocity) are studied. The reciprocal actions of two protrusions are investigated in complex model.The analysis parameters of models are shown in Table 1.

Table 1 Parameters in the analysis models

Parameters	Values / Unit
Tension of tape per unit width	15.5 N/m
Tape thickness	18.0 μm
Length of tape in complex model	60.0 mm
Length of tape in simple model	54.0 mm
Width of tape	12.6 mm
Young's modulus of tape	6.2 GPa
Poisson's ratio of tape	0.3
Relative velocity	5.8 m/sec
Mean free path of air molecule	64.0 nm
Air viscosity	18.1 μPa·sec
Atmospheric pressure	0.101325 MPa
Radius of cylinder	31.0 mm
Radius of pro.	11.0 mm
Height of pro. in simple model	21.0 μm
Height of pro. in complex model	31.0 μm
Angle between pros.	30.0 deg.

*) pro. : protrusion

3.1 Parameter study in a simple model

The simple model of numerical simulation is shown in Fig. 2.

The tape on drum is sustained by posts. The analysis domain is the region between both posts near drum. The contact between post and tape is described by applying proper boundary condition at both ends of the tape. The pressure boundary condition to the edge of tape(a-b-c-d) is chosen as atmospheric pressure boundary condition. The simply-supported boundary condition to the edge(a-b,c-d) of tape and the free edge boundary condition to the edge(b-c,d-a) are applied. The

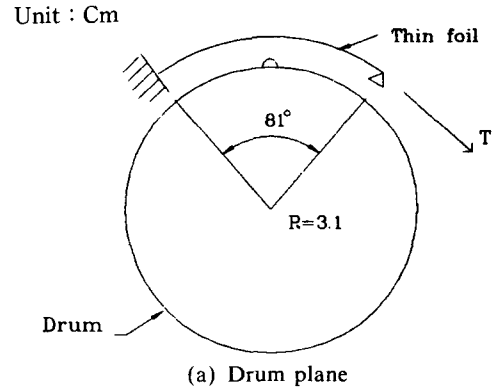

Fig. 2 Numerical model of tape and drum with the boundary conditions in simple model with one protrusion

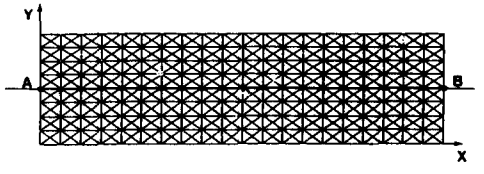

Fig. 3 Finite element mesh for tape and air gap discretized with triangular elements in simple model

proper tension is loaded to the edge(c-d). Initial shape of tape is given as cylindrical plane which has radius of drum including the adequate spacing. Initial value of lubrication pressure is atmospheric pressure over the entire domain. The discretization of tape of simple model is shown in Fig.3. To solve the global equations, the number of iteration is needed to 30~40 iterations in case that convergence indicator ε is chosen below 10^{-3} ~ 10^{-4}.

3.1.1 Tension and vertical displacement of tape

Figure 4 shows the variation of vertical displacement along centerline of tape in Fig. 3

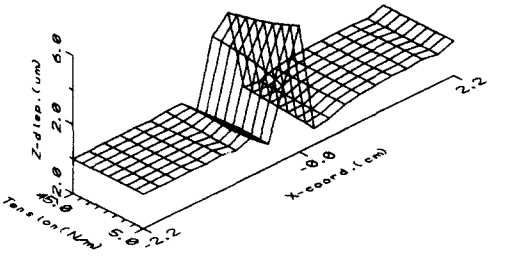

Fig. 4 Z-displacement of tape according to tension variation under the conditions that the protrusion is located at the center of analysis model and its height is 21μm.

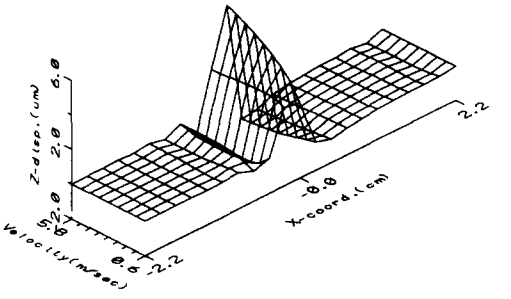

Fig. 5 Z-displacement of tape according to velocity variation under the conditions that the protrusion is located at the center of analysis model and its height is 21μm.

where the tension varies from 5(N/m) to 45(N/m) by the 5(N/m) with 21(μm) point protrusion at the center of drum in analysis model. As the tension increases, the positive and the negative vertical displacement of tape decrease around the protrusion. This means stiffness of the tape increase according as the tension increase. Also, the range of the vertical displacement near protrusion varies linearly to the increase of the tension.

3.1.2 Relative velocity and vertical displacement of tape

Figure 5 shows the variation of vertical displacement along center line (A-B) in Fig. 3 where drum velocity varies from 0.6(m/sec) to 5.8(m/sec) by the 0.65(m/sec) with 21(μm) point protrusion at the center of the drum. Maximum displacement occurs at the top point of the protrusion and the negative displacement is larger at the rearside of protrusion than at the frontside. As the velocity increases, the vertical displacement of

tape increases. This shows that the pressure of air gap increases as the velocity increases.

3.2 The reciprocal action of two protrusions in a complex model

The complex analysis model is shown in Fig. 6. The tape is running over drum with multiple protrusions along the centerline of drum. The analysis parameters are shown in Table 1. The Fig. 7 shows the topology of elements in analysis domain of tape and air gap. The minimum resolutions of mesh in x and y direction are 0.35 mm and 0.26 mm respectively.

The overall view of the tape displacement is presented in Fig. 8 with mutiple protrusions, front protrusion and rear protrusion with the angle difference of $\Theta=30°$. The displacement of tape and the pressure of air gap are shown along the tape centerline of protrusion path in Fig. 9. The spacing around the rear protrusion is a little smaller than the one around the front protrusion as shown in Fig. 10. In Fig. 11, considering the in-plane displacement in width direction(shrinkage) of the tape along the tape edge, the shrinkage at the region of protrusion is larger than that at the other region.

In nonlinear analysis, there is a close correlation between the number of iteration and relaxation factor. By selecting relaxation factors with respect to the magnitude of convergence indicator,

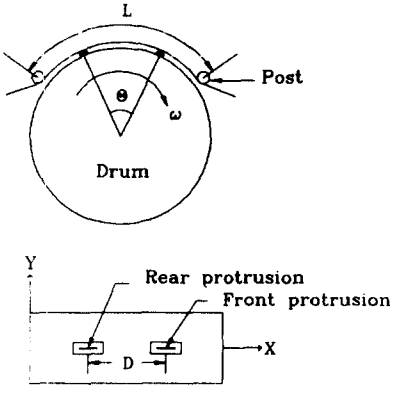

L : Thin foil length
θ : Angle between rear and front protrusion
D : Length between rear and front protrusion
ω : Relative angular velocity

Fig. 6 Numerical model of tape and drum with two protrusions in complex model

Fig. 7 Finite element mesh for tape and air gap discretized with triangular elements in complex model

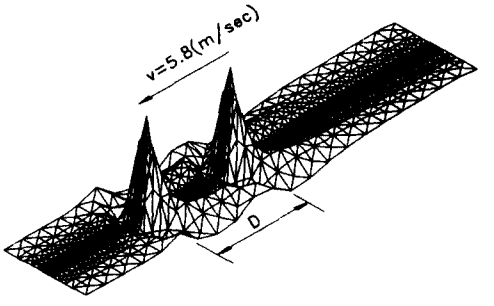

Fig. 8 3-dimensional profile of z-displacement of tape in two protrusions system

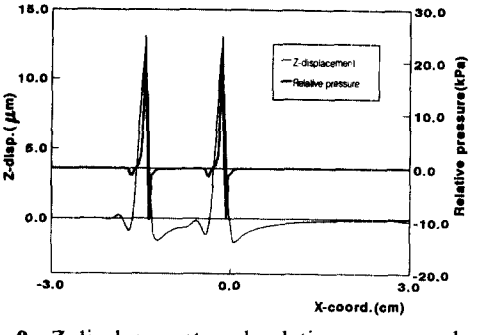

Fig. 9 Z-displacement and relative pressure along the centerline of protrusion path

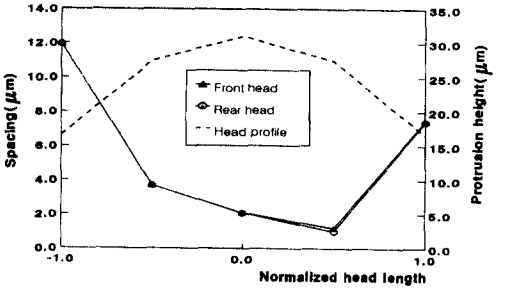

Fig. 10 Spacing on the centerline of protrusion path at the front and rear protrusions

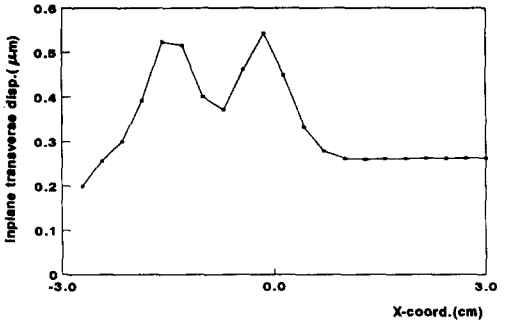

Fig. 11 Inplane displacement in tape width direction(shrinkage) along the tape edge

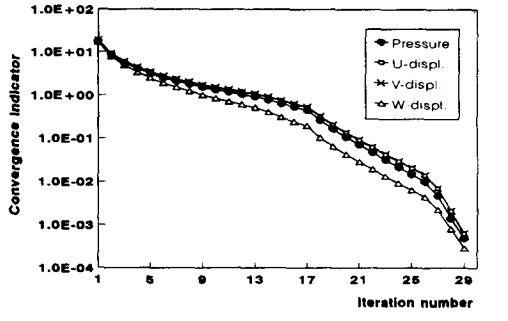

Fig. 12 Convergence indicator and iteration number

the number of iteration is fairly reduced to 30~40 iterations as shown in Fig. 12. Numerical model for this nonlinear analysis was simulated by using Cray Y-MP4/116 system under the Unicos 6.0.

4. Conclusion

The elasto-hydrodynamic mechanism of the running tape and the rotating drum with protrusion is analyzed numerically. Using the finite element method and Newton-Raphson method as a numerical schemes, a numerical algorithm is developed to analyze the displacement and pressure distribution of tape based on the coupled nonlinear equations. To understand the characteristics of tape over the entire region as well as near the protrusion, the large region of tape and air gap is chosen with the proper boundary conditions. From the results of nonlinear FEM analysis about flying characteristics of tape running on protrusion(s) on drum, the conclusions are :

(1) The effects of the tension and the magnitude of vertical displacement

As the tension increases, the positive and negative vertical displacement of tape decreases at the front of protrusion. This means the global stiffness of tape increases as the tension increases. Also, this shows the range of vertical displacement near the protrusion linearly decreases as to the increase of tension.

(2) The effects of the drum velocity and the magnitude of vertical displacement

Maximum displacement occurs at the top point of protrusion and negative displacement is larger at the rear than at the front of protrusion. At the rear of protrusion the region of displacement is long. As the velocity increase, the positive vertical displacement of tape increases but the negative vertical displacement decreases. This indicates pressure of air lubrication layer increases as the velocity increases.

(3) The reciprocal action of the two protrusions

Maximum displacement is almost the same at the top of both protrusion. But the spacing is smaller at the rearside than at the frontside in front or rear protrusions.

Formulation and simulation for the flying characteristics of the tape over the protrusion presented in this paper may be applicable to the analysis of mechanical conditions for digital VCR, which requires high frequency signal transmission. Especially, the allocation and dimension of the protrusions on the drum may be simulated and determined through this method.

Acknowlegement

The authors would like to express their appreciation to the Korea Science and Engineering Foundation for supporting this research. They have also owed Kia Motors Corporation for computer resources and GoldStar Corporation Ltd. for supporting the experimental models.

References

Wolf, B., Deshpande, N. and Castelli, V., 1983, "The Flight of a Flexible Tape Over a Cylinder

with a Protruding Bump," Journal of Lubrication Technology, Transaction of ASME, Vol. 105, pp. 138~142.

Kotera, H., Kita, H., Yohda, H. and Mizoh, Y., 1991, "Finite Element Analysis of the Interface Phenomena Between VCR Tape and Head," IEEE Trans. Mag., Vol. 27, pp. 224~227.

Sakai, K., Terayama, T., Morikawa, T. and Ohawada, N., 1990, "Study on Head-tape Interference in VCR's," JSME Int. Jour. Vol. 33, No. 4, pp. 655~662.

Kim, S., Min, O. and Kwon, H., 1992, "Flying Characteristics of Tape Above Rotating Drum with Multiple Heads," IEEE Trans. Con. Elect., Vol. 38, No. 3, pp. 671~673.

Yoneda, K. and Sawada, T., 1987, "Simulation of Spacing Between Magnetic Protrusion and Medium on Video Floppy," IEEE Trans. Journal of Mag. Vol. TJMJ-2, pp. 490~496.

Yoneda, K. and Sawada, T., 1988, "Simulation of Tape Flying Characteristics on VTR Drum Considering In-plane Stress," IEEE Trans. Mag., Vol. 24, No. 6, pp. 2766~2768.

Min, O. and Kim, S., 1991, "Flying Characteristics of Running Tape Above Rtating Protrusion(I)," Jounrnal of Korean Society of Mechanical Eng. Vol. 15, No. 2, pp. 523~536.

Giro, S., Bukan, S. and Yashi, H., 1969, "2-D Hydrodynamic Lubrication Theory of Foil Bearing," Japanese Society of Mechanical Eng(3), Vol. 35, No. 276, pp. 1781~1787.

Langlois, W. E., 1975, "Finite Width Foil Bearing with Light Loading," Journal of Applied Mechanics, Transactions of the ASME, pp. 274~278.